A Chloride-doped Cu_{18} Nanocluster: Synthesis, Bonding and Nonlinear Optical Property

Xuekun Gong[+a], Chan Zheng[+b], Dongjie Zuo[+a], Simin Li[a]*, Wei-Hui Fang[c]*, and Hui Shen[a]*

[a] College of Energy Materials and Chemistry, Inner Mongolia University, Hohhot 010021, China

[b] Institute of Biology and Chemistry, Fujian University of Technology, 350118, Fuzhou, P.R. China

[c] State Key Laboratory of Structural Chemistry, Fujian Institute of Research on the Structure of Matter, Chinese Academy of Sciences, Fuzhou, Fujian, 350002, P.R. China

[+]These authors contributed equally to this work

E-mail: shen@imu.edu.cn; fwh@fjirsm.ac.cn

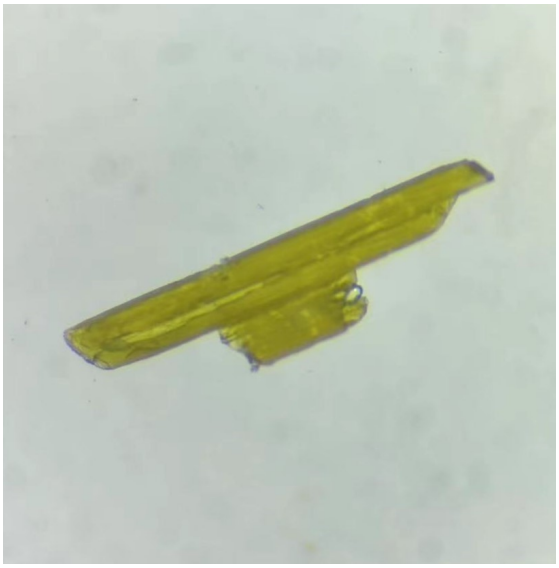

Figure S1. Digital photograph of single crystals of $ClCu_{18}$ clusters under the microscope.

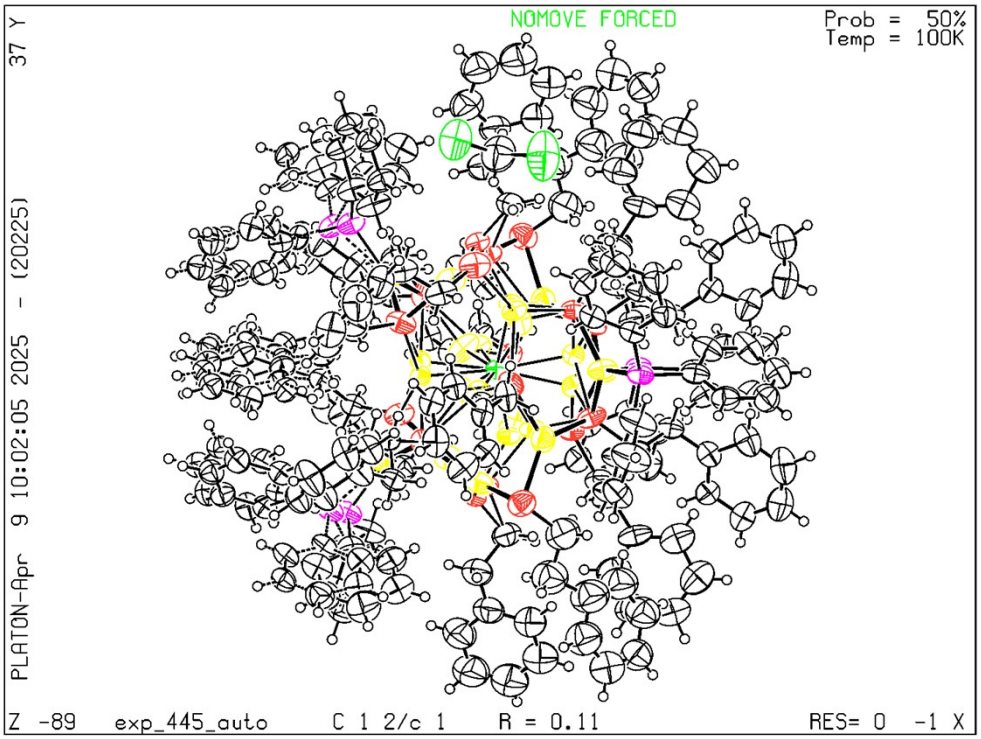

Figure S2. ORTEP diagram of $ClCu_{18}$ with the thermal ellipsoids at 50% probability.

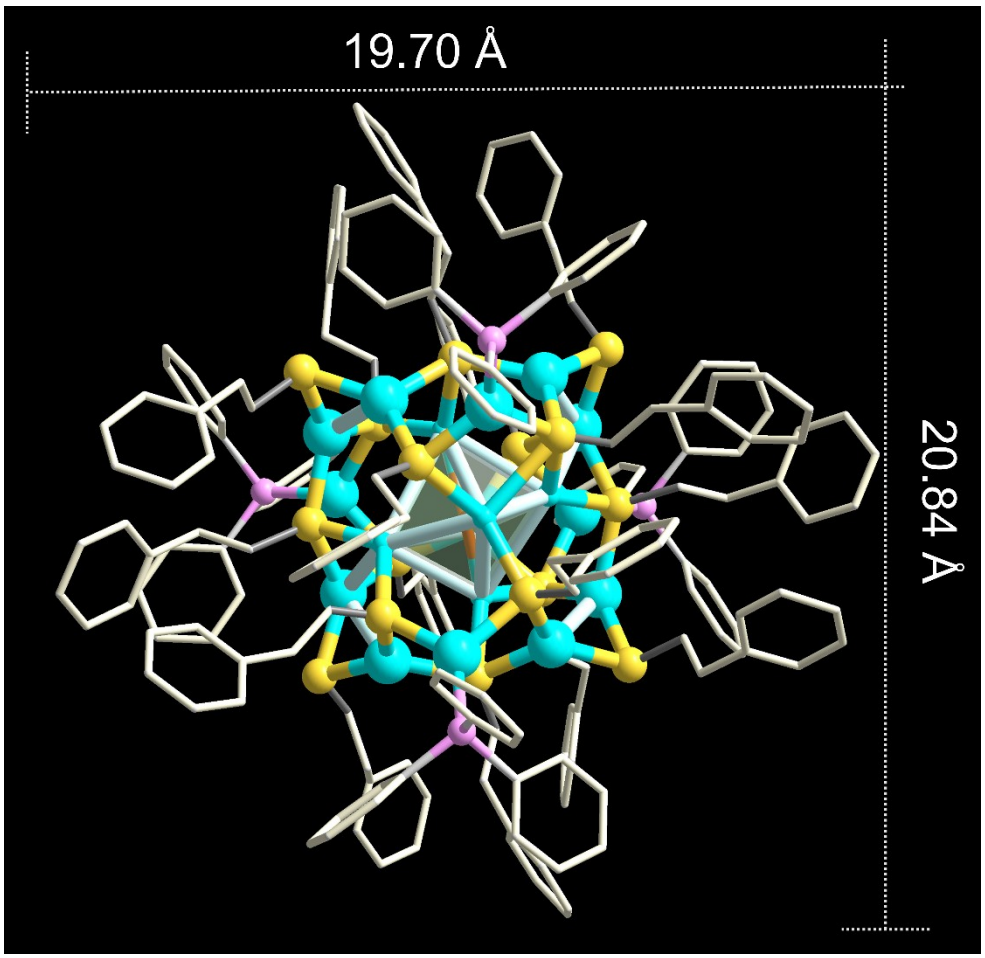

Figure S3. The overall $ClCu_{18}$ cluster diagram of length and width.

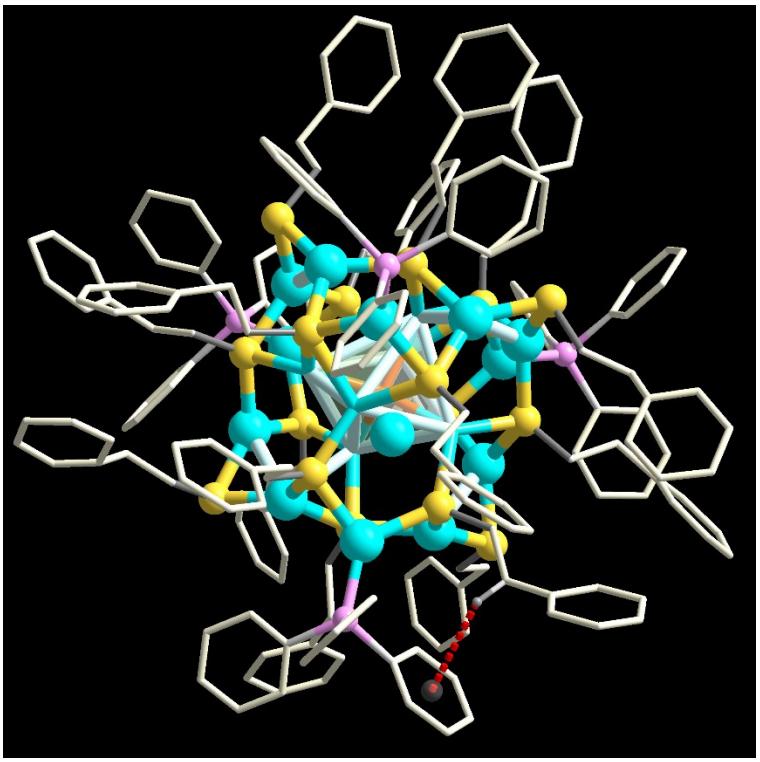

Figure S4. The C-H···π interactions in $ClCu_{18}$ (highlighted as red dashed line). Color legends: Cu blue; S yellow; P pink; Cl orange; C gray. Hydrogen atoms are omitted for clarity.

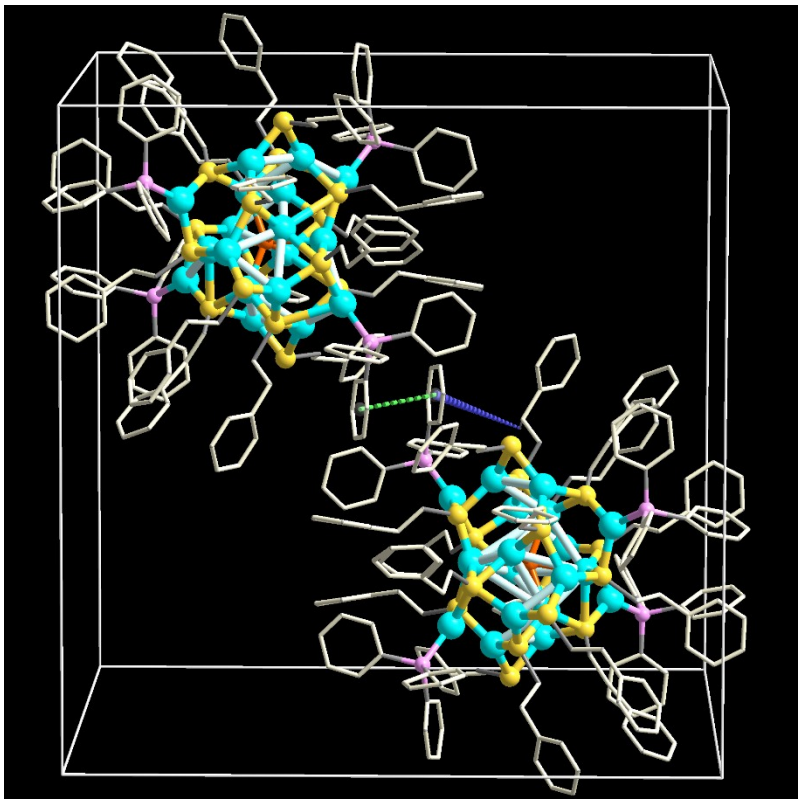

Figure S5. The C-H···π···π interactions in the packing structure of the $ClCu_{18}$ cluster in their single crystals (highlighted as green and purple dashed lines). Color legends: Cu blue; S yellow; P pink; Cl orange; C gray. Hydrogen atoms are omitted for clarity.

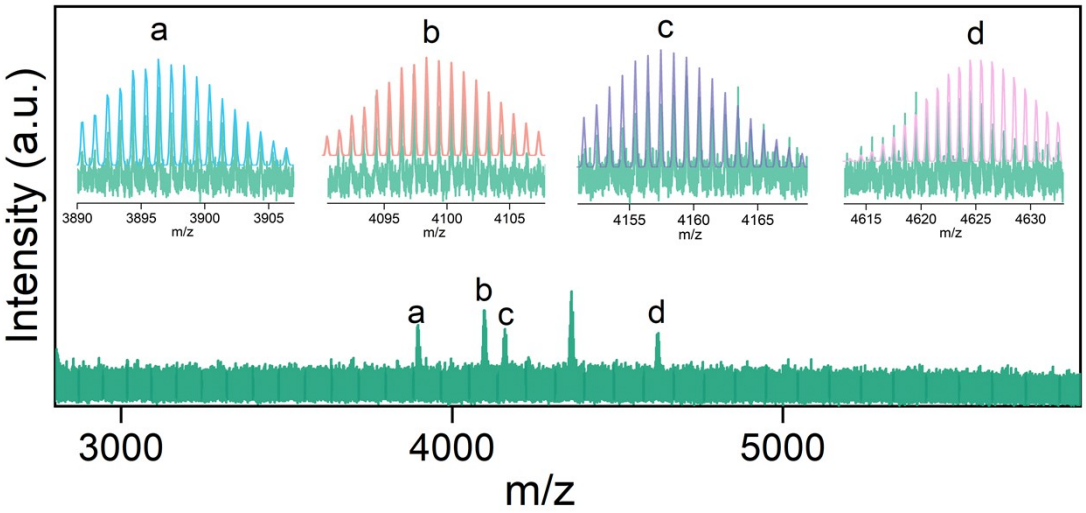

Figure S6. The ESI-MS spectrum of the $ClCu_{18}$ cluster. Inset are the comparisons between experimental and simulated isotopic patterns of peaks a: $([Cu_{18}(PET)_{16}Cl(PPh_3)(CH_2Cl_2)_2(H_2O)]^+)$, b: $([Cu_{18}(PET)_{16}Cl(PPh_3)_2(CH_2Cl_2)_2(CH_3OH)]^+)$, c: $([Cu_{18}(PET)_{16}Cl(PPh_3)_1(CH_2Cl_2)_2(CH_3OH)(BPh_4)H]^+$ and d: $([Cu_{18}(PET)_{16}Cl(PPh_3)_4(CH_2Cl_2)_2(CH_3OH)]^+)$.

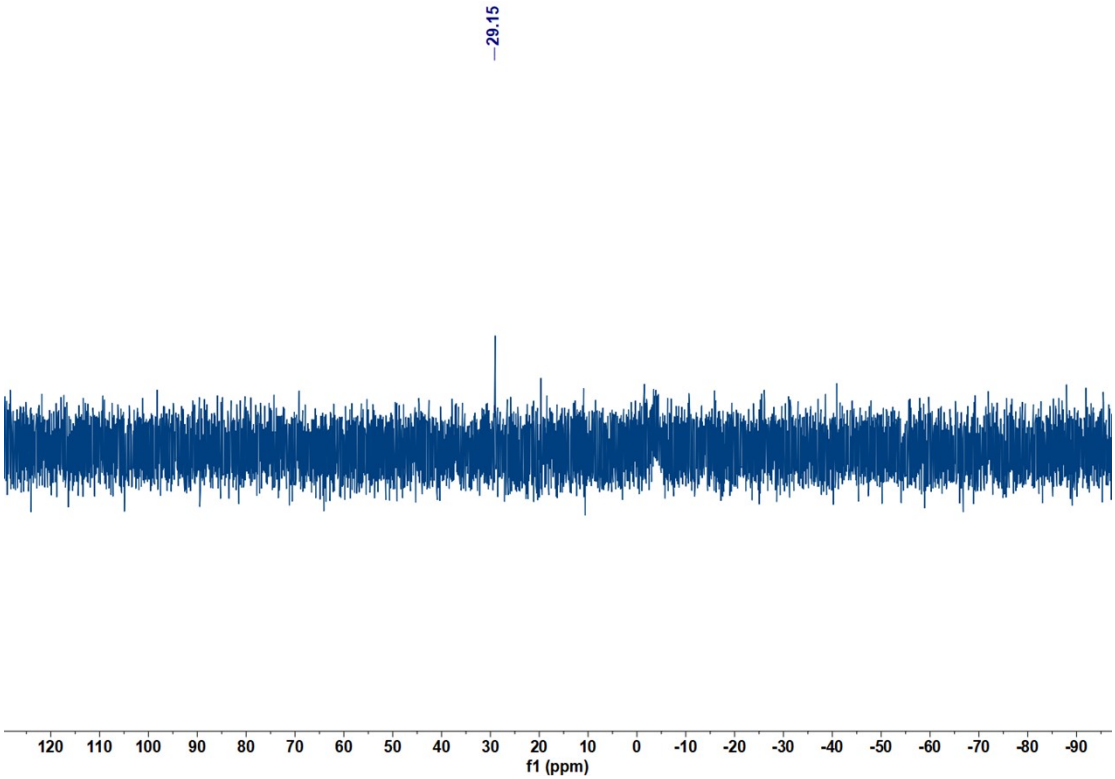

Figure S7. The proton-decoupled ^{31}P NMR spectrum of $ClCu_{18}$ in $CDCl_3$.

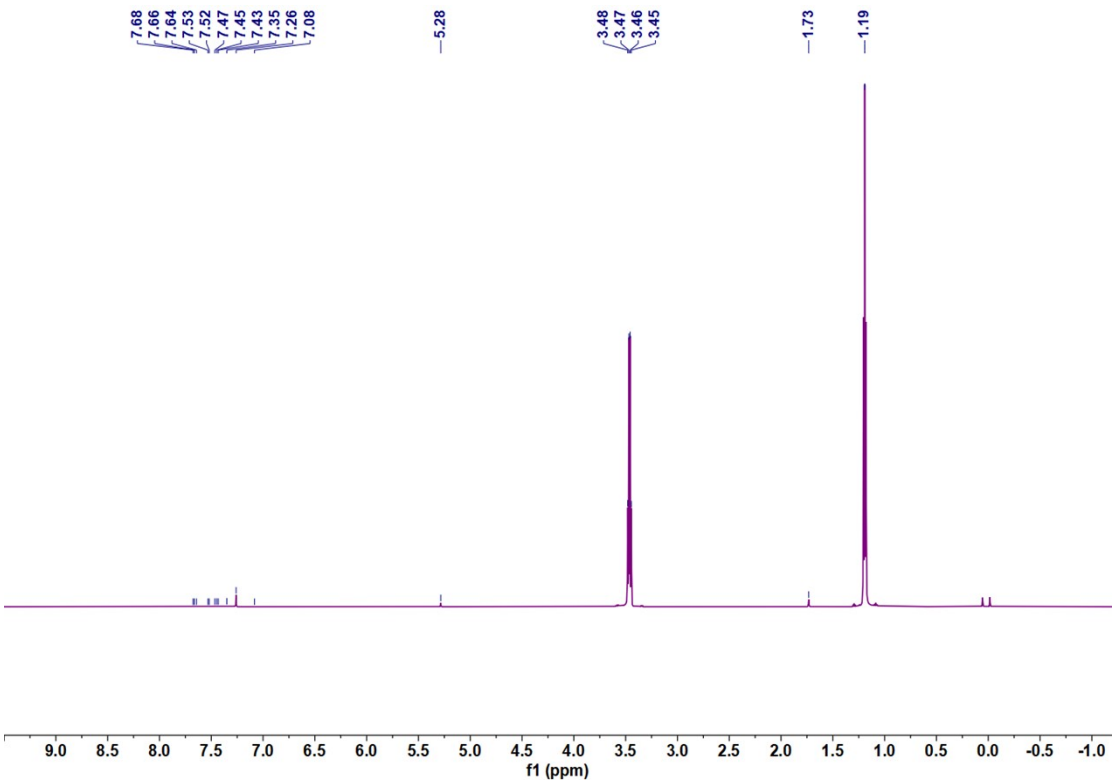

Figure S8. The ^{1}H NMR spectrum of $ClCu_{18}$ in $CDCl_3$.

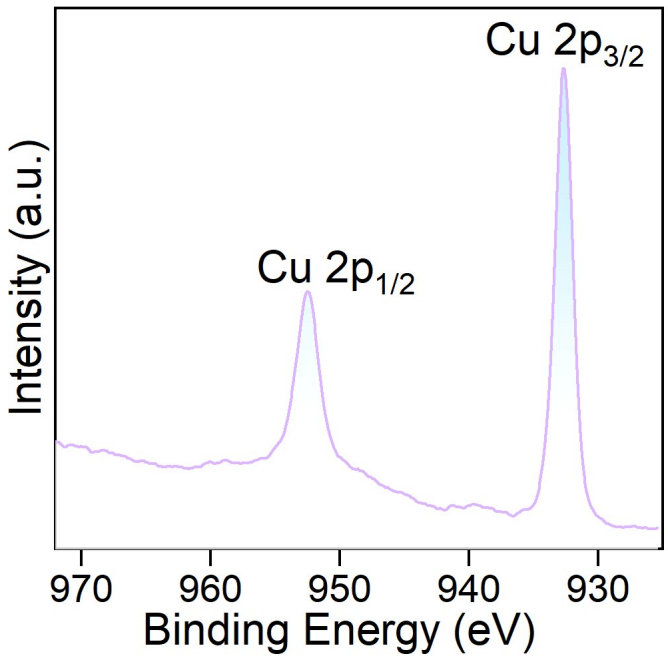

Figure S9. The initial XPS data of Cu 2p of the $ClCu_{18}$ cluster.

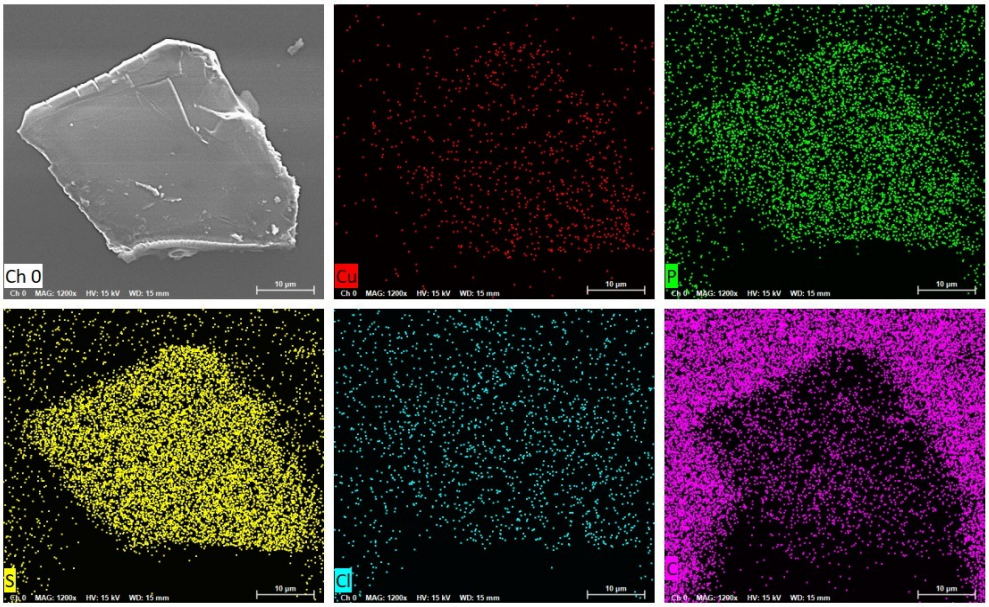

Figure S10. The EDS elemental maps of the $ClCu_{18}$ cluster.

Table S1. Crystal data and structure refinement for $ClCu_{18}$.

Compound	$[ClCu_{18}(C_8H_9S)_{16}(C_{18}H_{15}P)_4(CH_2Cl_2)]^+$
CCDC No.	2442407
Formula	$C_{202}H_{208}Cu_{18}Cl_5P_4S_{16}$
Formula weight	4593.48
Temperature/K	100.01(10)
Crystal system	monoclinic
Space group	*C2/c*
a (Å)	27.4052(3)
b (Å)	27.2127(4)
c (Å)	27.7815(4)
α (˚)	90.0(10)
β (˚)	92.0930(10)
γ (˚)	90.0(10)
V ($Å^3$)	20704.8(5)
Z	4
D_c / ($g \cdot cm^{-3}$)	1.474
Radiation	Cu Kα (λ = 1.54184)
2Theta (˚) range	4.578 to 155.47
Index ranges	$-34 \leq h \leq 34$, $-32 \leq k \leq 34$, $-32 \leq l \leq 35$
Refls. Total	99385
Restraints	703
Parameters	1268
R_{int}	0.0692
R_1/wR_2 [I>2σ(I)]	0.1101/0.3417
R_1/wR_2 (all data)	0.1468/0.3924
Goodness-of-fit on F^2	1.300

Table S2. Selected bond lengths (Å) for compound $ClCu_{18}$.

Parameter	value	Parameter	value
Cu2-Cu6	2.958(2)	Cu57-S5	2.440(5)
Cu2-S13[1]	2.290(2)	Cu57-S58	2.056(5)
Cu2-S2	2.273(2)	Cu3-S5	2.254(2)
Cu4-Cu8	2.626(9)	Cu3-S1	2.258(3)
Cu4-S1	2.240(3)	Cu3-P13	2.070(8)
Cu4-S10	2.244(2)	Cu3-P1	2.397(10)
Cu4-S9[1]	2.441(5)	Cl53-Cu54	2.287(2)
Cu4-Cu1[1]	2.564(3)	Cl53-Cu54[1]	2.287(2)
Cu4-S8[1]	2.192(5)	Cl53-Cu12	2.553(3)
Cu4-Cu9	2.815(9)	Cl53-Cu1	2.309(2)
Cu8-S13	2.356(9)	Cl53-Cu5	2.478(3)
Cu8-S58[1]	2.366(8)	Cl53-Cu10	2.285(6)
Cu8-S10	2.072(2)	Cl53-Cu10[1]	2.285(6)
Cu6- Cu7	2.740(2)	Cu54-S13[1]	2.205(3)
Cu6-Cu57	2.673(4)	Cu54-S2[1]	2.737(4)
Cu6-S2	2.223(3)	Cu54-Cu12	2.847(4)
Cu6-S58	2.287(3)	Cu54-S9	2.316(6)
Cu6-S11	2.218(3)	S13-Cu12	2.406(2)
Cu7-S5	2.272(3)	S13-Cu1[1]	2.523(3)
Cu7-S11	2.224(3)	S13-Cu9	2.157(10)
Cu7-S9[1]	2.104(5)	S2-Cu12	2.160(3)
Cu7-Cu1[1]	3.052(3)	S5-Cu10	2.144(6)
Cu7-S8[1]	2.446(5)	S1-Cu5	2.163(3)
Cu7-Cu10	3.048(7)	S58-Cu9[1]	2.111(9)
Cu57-Cl53	2.281(6)	S58-Cu10	2.469(5)
S10-Cu9	2.437(7)		

Table S3. Refractivity (n_0), linear absorption coefficient (α), nonlinear absorption coefficient (β), the imaginary part of third-order nonlinear susceptibility ($\chi^{(3)}$), FOM, and the onset of OL of the $ClCu_{18}$ cluster at different pulse energies, respectively.

	n_0	α_0 (cm^{-1})	β (*10^{-10} m/W)	Im$\chi^{(3)}$ (*10^{-12} esu)	FOM (*10^{-12} esu)
20μJ	1.33	2.31	1.60	4.52	1.96
40μJ	~	~	1.66	4.69	2.03
60μJ	~	~	1.70	4.80	2.08
75μJ	~	~	1.72	4.86	2.1

Table S4. The comparison of nonlinear optical properties among different Cu nanoclusters.

Cluster	Ligand	β (cm/GW)	Reference
$ClCu_{18}$	2-penylethylmercaptan	17.2 (this work)	This work
Cu_{50}-1	3,5-*di*Me-PhSH	96.3	*ACS Materials Lett.* 2024, 6, 281
Cu_{50}-2	4-F-PhSH	25.6	*ACS Materials Lett.* 2024, 6, 281
Cu_{50}-3	PhSH	32.1	*ACS Materials Lett.* 2024, 6, 281
Cu_{50}-4	4-F-PhSH	12.5	*ACS Materials Lett.* 2024, 6, 281
Cu_{25}	2-fluorobenzenethiol	13.8	*Polyoxometalates*, 2025, 4, 9140072
Cu_{26}	2-fluorobenzenethiol	23.1	*Polyoxometalates*, 2025, 4, 9140072